J. Am. Chem. Soc. **1996,** *118,* 401−406

Probing Hydrogen Bonding and the Local Environment of Silanols on Silica Surfaces via Nuclear Spin Cross Polarization Dynamics

I-Ssuer Chuang and Gary E. Maciel*

Contribution from the Department of Chemistry, Colorado State University,
Fort Collins, Colorado 80523-0002

Received May 12, 1995⊗

Abstract: By studying $^{1}H \rightarrow ^{29}Si$ cross-polarization dynamics of two untreated and two "dry" silica gel samples (one evacuated at 25 °C and one evacuated at 200 °C), we find that all the surface silanols on the two untreated silicas are hydrogen bonded, either to the hydroxyl groups of adjacent silanol(s) or to water molecule(s). About 46% and 47% of the geminal silanols and 53% and 58% of the single silanols that were hydrogen bonded only to water in the two untreated silicas become non-hydrogen bonded on the two "dry" silica surfaces, but the remainder of the silanols of the untreated silicas (i.e., those hydrogen bonded to other silanols) remain hydrogen bonded to other silanols upon drying. The ratio of the number of hydrogen-bonding single silanols to the number of hydrogen-bonding geminal silanols is 17-to-1 for a Fisher silica surface evacuated at 25 °C and 16-to-1 for a Baker silica surface evacuated at 200 °C. These results can be explained in terms of a generalized silica surface model based on the β-cristobalite crystal structure.

Introduction

Silicas and modified silicas are highly versatile materials with numerous applications, such as catalysis, separation science, microelectronics, consumer products, and composite materials. Many applications of silicas rely on their unique surface properties, which in turn are largely determined by the concentration, distribution, and nature of hydroxyls (silanols) on the surface.[1,2] Various NMR techniques,[3−18] infrared[3−6,15,19−24] and Raman[21,24,25] spectroscopies, chemical probes,[3,4,11,12,19−21] and various other analytical tools[1−3,19,26] have been utilized to investigate hydroxyls on silica surfaces.

The characterization of cross-polarization[27] (CP) spin dynamics[14,27−31] is not only a must for reliable quantitation in a CP-MAS NMR experiment,[32] but it also can provide a rough estimate for heteronuclear dipolar interaction strengths,[14,28−31] which are related to chemical structure (internuclear distances) and dynamics. In a previous article,[17] we indicated that for the ^{29}Si nuclei of isolated single silanols the cross-polarization time constant, T_{HSi} (*vide infra*), is at least five times larger than that for hydrogen-bonded single silanols. Therefore, by ^{29}Si CP-MAS NMR spectroscopy it is possible to distinguish hydrogen-bonded silanols from non-hydrogen-bonded silanols and at the same time to quantify the ratio of geminal silanols and single silanols on a silica surface under various conditions (e.g., untreated or evacuated at various temperatures). In that previous article, we also established that *both* geminal silanols and single silanols exist and are not hydrogen bonded on a silica surface that has been evacuated at 500 °C.

In this article, we show how the characterization of CP spin dynamics can be employed to probe hydrogen bonding and the local structural environments of various hydroxyl groups of silica surfaces in greater detail. We also show that a generalized

---

⊗ Abstract published in *Advance ACS Abstracts,* December 15, 1995.

(1) Iler, R. K. *The Chemistry of Silica*; Wiley: New York, 1979.

(2) Brinker, C. J.; Scherer, G. W. *Sol-Gel Science: The Physics and Chemistry of Sol-Gel Processing*; Academic Press: New York, 1990.

(3) Köhler, J.; Chase, D. B.; Farlee, R. D.; Vega, A. J.; Kirkland, J. J. *J. Chromatogr.* **1986**, *352*, 275.

(4) Davydov, V. Y.; Kiselev, A. V.; Pfeifer, H.; Junger, I. *Russ. J. Phys. Chem.* **1983**, *57*, 1527.

(5) Haukka, S.; Lakomaa, E.-L.; Root, A. *J. Phys. Chem.* **1993**, *97*, 5085.

(6) Haukka, S.; Root, A. *J. Phys. Chem.* **1994**, *98*, 1695.

(7) Bronnimann, C. E.; Zeigler, R. C.; Maciel, G. E. *J. Am. Chem. Soc.* **1988**, *110*, 2023.

(8) Kinney, D. R.; Chuang, I-S.; Maciel, G. E. *J. Am. Chem. Soc.* **1993**, *115*, 6786.

(9) Maciel, G. E.; Sindorf, D. W. *J. Am. Chem. Soc.* **1980**, *102*, 7606.

(10) Sindorf, D. W.; Maciel, G. E. *J. Am. Chem. Soc.* **1983**, *105*, 1487.

(11) Sindorf, D. W.; Maciel, G. E. *J. Phys. Chem.* **1982**, *86*, 5208

(12) Maciel, G. E.; Bronnimann, C. E.; Zeigler, R. C.; Chuang, I-S.; Kinney, D. R.; Keiter, E. A. In *The Colloid Chemistry of Silica*; Bergna, H. E., Ed.; Advances in Chemistry Series 234, American Chemical Society: Washington, DC, 1994; p 269.

(13) Chuang, I-S.; Kinney, D. R.; Bronnimann, C. E.; Zeigler, R. C.; Maciel, G. E. *J. Phys. Chem.* **1992**, *96*, 4027.

(14) Walther, K. L.; Wokaun, A.; Baiker, A. *Mol. Phys.* **1990**, *71*, 769.

(15) Legrand, A. P.; Hommel, H.; Tuel, A.; Vidal, A.; Balard, H.; Papirer, E.; Levitz, P.; Czernichowski, M.; Erre, R.; Van Damme, H.; Gallas, J. P.; Hemidy, J. F.; Lavalley, J. C.; Barres, O.; Burneau, A.; Grillet, Y. *Adv. Colloid Interface Sci.* **1990**, *33*, 91.

(16) Tuel, A.; Hommel, H.; Legrand, A. P.; Chevallier, Y.; Morawski, J. C. *Colloids Surf.* **1990**, *45*, 413.

(17) Chuang, I-S.; Kinney, D. R.; Maciel, G. E. *J.. Am. Chem. Soc.* **1993**, *115*, 8695.

(18) Maciel, G. E.; Ellis, P. D. in *NMR Techniques In Catalysis*, Bell, A. T.; Pines, A., Eds.; Marcel Dekker: New York, 1994; p 231.

(19) Peri, J. B. *J. Phys. Chem.* **1966**, *70*, 2937.

(20) Hair, M. L. *Infrared Spectroscopy In Surface Chemistry*; Marcel Dekker: New York, 1967.

(21) Morrow, B. A.; McFarlan, A. J. *J. Non-Cryst. Solids* **1990**, *120*, 61.

(22) Hoffmann, P.; Knözinger, E. *Surf. Sci.*, **1987**, *188*, 181.

(23) Kiselev, A. V. *Discus. Faraday Soc.* **1971**, *52*, 14.

(24) Morrow, B. A.; McFarlane, R. A. *J. Phys. Chem.* **1986**, *90*, 3192.

(25) Brinker, C. J.; Tallant, D. R.; Roth, E. P.; Ashley, C. S. *J. Non-Cryst. Solids* **1986**, *82*, 117.

(26) Mikhail, R. S.; Robens, E. *Microstructure and Thermal Analysis of Solid Surfaces*; John Wiley & Sons: New York, 1983.

(27) Pines, A.; Gibby, M. G.; Waugh, J. S. *J. Chem. Phys.* **1973**, 59, 569.

(28) Mehring, M. *Principles of High Resolution NMR in Solids*, 2nd ed.; Springer-Verlag: New York, 1983.

(29) Klein Douwel, C. H.; Maas, W. E. J. R.; Veeman, W. S.; Buning, G. H. W.; Vankan, J. M. J. *Macromolecules* **1990**, *23*, 406.

(30) Eijkelenboom, A. P. A. M.; Maas, W. E. J. R.; Veeman, W. S.; Buning, G. H. W.; Vankan, J. M. J. *Macromolecules* **1992**, *25*, 4511.

(31) Slichter, C. P. *Principles of Magnetic Resonance,* 3rd ed.; Springer-Verlag: New York, 1989; p 79.

(32) Schaefer, J.; Stejskal, E. *J. Am. Chem. Soc.* **1976**, *98*, 1031.

0002-7863/96/1518-0401$12.00/0

model of silica surfaces based on β-cristobalite can account for our data.

Experimental Section

Fisher Scientific silica gel (S679−500; surface area: 456 m^2/g) was used directly without treatment (untreated Fisher) or with evacuation at 10^{-3} Torr at 25 °C for 24 h (Fisher evacuated at 25 °C). J. T. Baker silica gel (Analyzed Reagent, 34D5-01; surface area: 290 m^2/g) was used without treatment (untreated Baker) or with evacuation at 10^{-3} Torr and 200 °C (Baker evacuated at 200 °C). The untreated and 25 °C evacuated Fisher silica samples were loaded for ^{29}Si NMR measurements into 2.5 cm^3 "pencil"-type magic-angle spinning (MAS)[33,34] rotors (Chemagnetics) with zirconia sleeves. The untreated and 200 °C evacuated Baker silica samples were loaded for ^{29}Si NMR measurements into a Gay-type MAS rotor;[35] the Baker silica sample evacuated at 200 °C was sealed under reduced N$_2$ pressure in a glass tube to prevent moisture contamination.

^{29}Si NMR spectra were obtained at 39.75 MHz on a heavily-modified Nicolet NT-200 spectrometer under the conditions of ^{1}H−^{29}Si cross polarization, magic-angle spinning, and ^{1}H decoupling, using a 0.6 s repetition delay for the untreated Fisher and Baker silica samples, a 5 s repetition delay for the 25 °C evacuated Fisher sample, or a 6 s repetition delay for the 200 °C evacuated Baker sample. These repetition delays were chosen as apparently optimal for signal-to-noise ratio achieved within a specific time; these values are much too small to yield quantitative *absolute* intensities. However, since all the CP-MAS ^{29}Si signals of a specific sample yield the *same* proton spin−lattice relaxation time, T_1^{H} (see below), the choice of repetition delay does *not* impact on the quantitation of *relative* CP-MAS ^{29}Si signals *within* a given spectrum. The other conditions for CP-MAS experiments are described in the Results and Discussion section. The drive gas for MAS was air for the untreated Fisher and Baker samples and for the Baker sample evacuated at 200 °C and nitrogen for the Fisher silica evacuated at 25 °C. The radio frequency field strengths of both the ^{1}H and ^{29}Si channels were typically 30 kHz for the large-volume "pencil"-type MAS system and 40 kHz for the Gay-type system. ^{29}Si NMR chemical shifts are reported in ppm, referenced to liquid tetramethylsilane (by substitution), higher values corresponding to lower shieldings.

Measurements of T_1^{H} were made by a Freeman-Hill version of a CP-MAS T_1^{H} experiment, by detecting the ^{29}Si CP-MAS intensity that was cross polarized from protons.[36] The rotating-frame proton spin-lattice relaxation time ($T_{1\rho}^{\mathrm{H}}$) was measured by varying the duration of a ^{1}H spin-lock period prior to a fixed $^1\mathrm{H}\rightarrow{}^{29}\mathrm{Si}$ cross-polarization contact period (1 ms for Fisher samples and 5 ms for Baker samples). The cross-polarization time constants (T_{HSi}) were determined by analysis of variable contact-time experiments, using the independently-determined $T_{1\rho}^{\mathrm{H}}$ values in a nonlinear least-squares fit of the variable-contact-time data.

Relaxation parameters were derived in two ways: on the basis of (a) peak heights and (b) areas derived from spectral deconvolutions. The T_{HSi} data presented in this paper were based on deconvolutions (*vide infra*), but data analysis based on peak heights yielded substantially similar results (not given here). Since ^{29}Si-detected T_1^{H} and $T_{1\rho}^{\mathrm{H}}$ experiments produced sets of spectra for which peak shapes are invarient to variation in the relaxation period, peak heights were used to analyze these data.

Results and Discussion

With ^{29}Si in 4.7% natural abundance and the rather high proton density on the silica surface, the Hartmann-Hahn cross-polarized ^{29}Si NMR magnetization, $I(\tau)$, after a CP contact time τ can be described by[28]

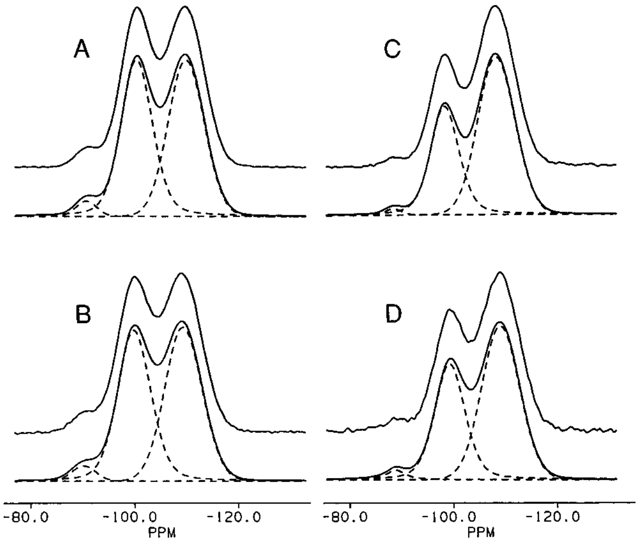

Figure 1. 39.75-MHz ^{29}Si CP-MAS spectra (upper) and their computer deconvolution simulations (lower) of the four samples of this study: A, untreated Fisher; B, Fisher evacuated; C, untreated Baker; D, Baker evacuated. CP contact time: 25 ms. MAS speed: 1.7 kHz (A, B), 2.2 kHz (C, D). Repetitions: 3000 (A), 1000 (B), 10000 (C), 2000 (D).

$$I(\tau) = \frac{I^*}{1-\lambda}(1 - \exp\{-(1-\lambda)\tau/T_{\mathrm{HSi}}\}) \exp\{-\tau/T_{1\varrho}^{\mathrm{H}}\} \qquad (1)$$

where I^* is the ideal (full) cross-polarized ^{29}Si magnetization and $\lambda = T_{\mathrm{HSi}}/T_{1\rho}^{\mathrm{H}}$. In eq 1, which is valid for the case $T_{1\rho}^{\mathrm{Si}} \gg T_{1\rho}^{\mathrm{H}}, T_{\mathrm{HSi}}$, the parameter T_{HSi}^{-1} is the ^{1}H−^{29}Si cross-polarization rate constant, which depends on the strength of the ^{1}H−^{29}Si and ^{1}H-^{1}H dipolar interactions and is roughly proportional to the inverse sixth power of ^{1}H−^{29}Si internuclear distance.[14,28−31] T_{HSi} and $T_{1\rho}^{\mathrm{H}}$ values vary with different samples and they may have different values for different sets of ^{29}Si and ^{1}H within a given sample. Therefore, for a quantitative analysis, T_{HSi} and $T_{1\rho}^{\mathrm{H}}$ must be determined for each peak.

Figure 1 shows ^{29}Si CP-MAS spectra of the four samples of this study, together with the computer deconvolution/simulation plots that represent the quality of deconvolutions used in the analysis of relaxation data. One sees, especially for the untreated samples (Figures 1A and 1C), the characteristic pattern of three peaks: a small peak (or shoulder) at −89 ppm due to Q$_2$ silicons, i.e., $(\geqslant\mathrm{SiO})_2\mathbf{Si}(\mathrm{OH})_2$; a peak at −99 ppm due to Q$_3$ silicons, i.e., $(\geqslant\mathrm{SiO})_3\mathbf{Si}\mathrm{OH}$; and a peak at −109 ppm due to Q$_4$ silicons, i.e., $(\geqslant\mathrm{SiO})_4\mathbf{Si}$.

For a reliable and simplified fitting of eq 1, $T_{1\rho}^{\mathrm{H}}$ values discussed in this article were measured independently, as described in the Experimental Section. For each of the silica samples of this study, essentially the same $T_{1\rho}^{\mathrm{H}}$ value was obtained for single silanol, geminal silanol, and siloxane silicons. The results for the four silica samples studied are summarized in Table 1.

In order to obtain the parameters I^* and T_{HSi} in eq 1, variable-contact-time (VCT) experiments were performed. For each of the two untreated silica samples (Fisher and Baker silicas), a single T_{HSi} value is sufficient to fit each set of VCT data for geminal silanols or for single silanols. However, two T_{HSi} values are needed for a satisfactory fit of the VCT data of geminal silanols or of single silanols of the two dry silica samples, the 25 °C evacuated Fisher silica and the 200 °C evacuated Baker silica. Derived T_{HSi} values and the corresponding relative

---

(33) Andrew, E. R. *Prog. NMR Spectrosc.* **1971**, *8*, 1.
(34) Lowe, J. J. *Phys. Rev. Lett.* **1959**, *2*, 285.
(35) Gay, I. D. *J. Magn. Reson.* **1984**, *58*, 413.
(36) Frye, J. S. *Concepts in Magn. Reson.* **1989**, *1*, 27.

Table 1. Relaxation Time Constants and Relative Contributions for Various Silicas, As Determined by ^{29}Si CP-MAS NMR

	T_{HSi} (ms) and relative contribution[a]		$T_1^{\mathrm{H}}\rho$ (ms)		T_1^{H} (s)	
	>Si(OH)$_2$ −89 ppm	⩾SiOH −99 ppm	>Si(OH)$_2$ −89 ppm	⩾SiOH −99 ppm	>Si(OH)$_2$ −89 ppm	⩾SiOH −99 ppm
Fisher untreated	1.3 (0.056)	2.0 (0.94)	42.8	43.7	0.3	0.3
Fisher evac at 25 °C	0.50 (0.027)	1.2 (0.45)				
			189	179	5	5
	6.0 (0.023)	14 (0.50)				
Baker untreated	1.2 (0.041)	2.1 (0.96)	36	36	0.09	0.09
Baker evac at 200 °C	0.49 (0.026)	1.4 (0.40)				
			163	169	5.5	5.7
	5.9 (0.023)	14 (0.55)				

[a] Fraction of contribution in parentheses.

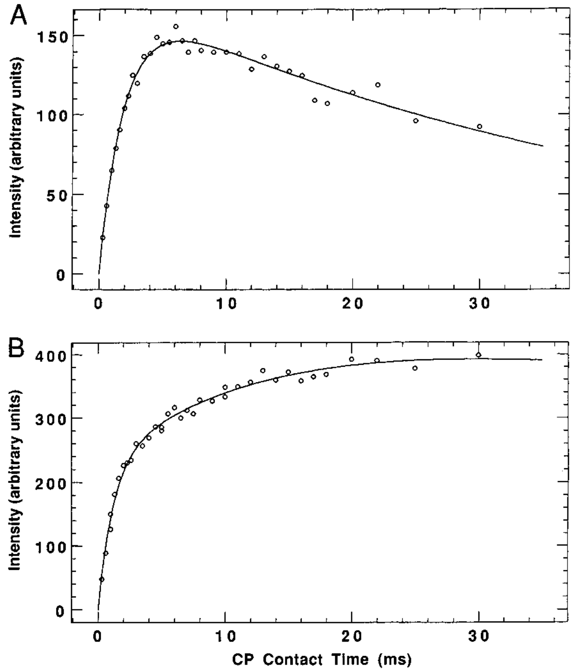

Figure 2. 39.75-MHz variable-contact-time ^{29}Si CP-MAS results and nonlinear least-square fits of the −99-ppm single-silanol peak for Fisher S-679 silica gel samples: (A) Untreated; (B) Evacuated at 10^{-3} Torr at 25 °C for 24 h. MAS speed 1.7 kHz. Repetitions: 3000 (A) or 1000 (B).

contribution of each T_{HSi} value for single silanols and for geminal silanols of the four silica samples are listed in Table 1, along with the corresponding $T_{1\rho}^{\mathrm{H}}$ and T_1^{H} values. Figures 2A and 2B show the computer fitting of the VCT peak intensity data representing single-silanol silicons on the surfaces of the untreated and 25 °C evacuated Fisher silicas, respectively. Even better fits (not shown here), also requiring two T_{HSi} values for each of the data sets representing the two dry silica samples, were obtained from data analysis in terms of peak heights.

On the basis of measured T_{HSi} values and ^{1}H−^{1}H and ^{1}H−^{29}Si dipolar-dephasing characteristics (the former prior to $^1\mathrm{H}\rightarrow{}^{29}\mathrm{Si}$ cross polarization), we previously indicated that internal (subsurface) single silanols have much smaller net ^{1}H−^{1}H and ^{1}H−^{29}Si dipolar interactions than those experienced by single silanols on the untreated silica surface.[17] We have shown that the T_{HSi} value for internal single silanols is roughly 4.5−5.0 times larger than T_{HSi} for external single silanols of untreated silica. This implies that the external single silanols of untreated silica experience ^{1}H−^{29}Si dipolar interactions that are slightly more than twice as large as those experienced for internal single silanols. On the surfaces of untreated silica gels, hydroxyl rotation of single silanols may be hindered or held rigidly through strong hydrogen bonding with water,[8,17] as shown symbolically in Figure 3A; in addition, some of the silanols can also be rendered rigid through strong hydrogen bonding with neighboring silanols (*vide infra*). For non-hydrogen-bonded internal single silanols that freely rotate about the Si−O bond axis, the ^{1}H−^{29}Si dipolar interaction within a given SiOH moiety would be scaled down by the factor[37] $(1/2)(3\cos^2 24° - 1) = 0.75$ (cf. Figure 3B), in comparison to single silanols on the untreated silica surface.

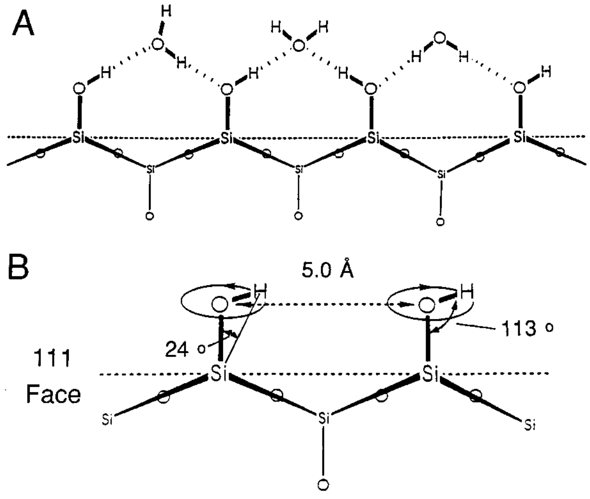

Figure 3. (A) Single-silanol surface structure with hydrogen bonding to water molecules. (B) Side view of the (111)-type plane (dotted line representing an edge of such a plane) of the β-cristobalite structure with a single silanol (drawn approximately to scale).

If the external single silanols on an untreated silica surface are held together relatively rigidly via hydrogen bonding to bridging water molecule(s) or neighboring silanols, then the protons of these nearby molecules also contribute to the overall extent of ^{1}H−^{29}Si dipolar interactions of the silicons of single silanols on the surface. Hence, hydrogen bonding can be expected to increase the *net* efficiency of $^1\mathrm{H}\rightarrow{}^{29}\mathrm{Si}$ cross polarization of single silanols relative to that of non-hydrogen-bonded single silanols by (1) increasing the number of protons that interact with each silanol silicon and (2) restraining motional averaging of the dipolar interactions. This overall differential

---

(37) Gutowsky, H. S.; Pake, G. E. *J. Chem. Phys.* **1950**, *18*, 162.

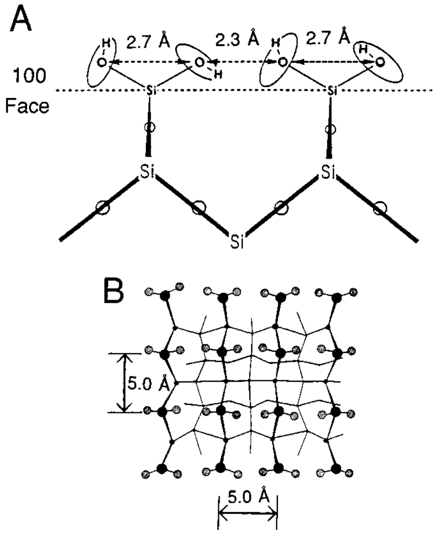

Figure 4. Representative (100)-type β-cristobalite face with geminal silanols (hydroxyl groups). (A) Side view of the (100)-type plane (dotted line representing an edge of such a plane) of the β-cristobalite structure with geminal silanols. (B) Top view of the (100)-type face (hydroxyl groups shaded; oxygen bridges not shown).

in CP efficiency makes it possible to distinguish between silanols with and without hydrogen bonds on the silica gel surface. The fact that just one T_{HSi} value is sufficient for fitting the VCT data for all single silanols and a different T_{HSi} value is sufficient for all geminal silanols on each of the untreated Fisher and Baker silicas indicates that the overall strengths of $^{1}\mathrm{H}-^{29}\mathrm{Si}$ dipolar interactions of each single silanol or geminal silanol are very similar to each other (within each silanol category), because all are involved in hydrogen bonding.

Previously, (111)-type and (100)-type faces of a β-cristobalite crystal structure, in which specific SiOSi moieties are replaced by SiOH moieties, have been discussed as models for surfaces containing single silanols and geminal silanols, respectively, of silicas.[1,2,10,11] According to this model and the discussion above, single silanols on a given (111)-type face of an undried silica sample are "bridged" via hydrogen bonding to water molecules. Adjacent geminal silanols on the same (100)-type face of an untreated silica surface are close enough together, with proper relative orientation, to form hydrogen bonds with each other (Figure 4A). Figure 4B is a top view of a (100)-type face; the hydroxyl groups on adjacent geminal silanols in the same row point toward each other, with a spatial relationship identical to that of the inner pair of hydroxyl groups in Figure 4A, and can hydrogen bond with each other. However, the hydroxyl groups on adjacent geminal silanols in the same column of Figure 4B have a similar spatial relationship to that of adjacent single silanols on the same (111)-type face (see Figure 3B) and cannot hydrogen bond with each other. On an untreated silica surface, the adjacent geminal silanols in the same column of Figure 4B are bridged via hydrogen bonding to water molecules, similar to the situation for single silanols on the same (111)-type face (cf. Figure 3A).

The fact that two T_{HSi} values are needed to fit the VCT results for peak intensities representing single silanols and two values are needed to fit the data for geminal silanols of both *dry* samples (Fisher and Baker silicas evacuated at 25 and 200 °C, respectively) implies that the $^{1}\mathrm{H}-^{29}\mathrm{Si}$ dipolar interactions of various single silanols have different magnitudes, and the same thing is true for the various geminal silanols. For single silanols of the dry (25 °C evacuated) Fisher sample, the large T_{HSi} value (14 ms) is almost identical to the T_{HSi} value reported for interior hydroxyl groups (non-hydrogen-bonding single silanols) in a previous article;[17] therefore, the $T_{\mathrm{HSi}} = 14$ ms set of single silanols can be attributed to non-hydrogen-bonded single silanols. The single silanols with a 1.2 ms T_{HSi} value can be attributed to hydrogen-bonded single silanols. Similarly, those geminal silanols with a large T_{HSi} value (6 ms) are identified here as *not* hydrogen bonded; those geminal silanols with $T_{\mathrm{HSi}} = 0.5$ ms are identified as involved in hydrogen bonding. It is presumably not coincidental that for each category of silanols, there is roughly a factor of 2 between the T_{HSi} values of single and geminal silanols.

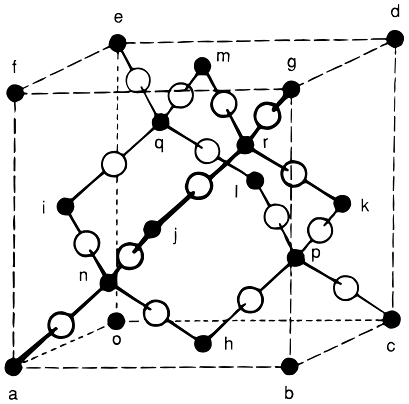

Figure 5. Unit cell of the β-cristobalite crystal structure, according to Wells.[39] Solid circles represent silicon sites and open circles oxygen sites. The Si−O−Si angle is 147° and each silicon is connected to four other silicons tetrahedrally through oxygen bridges.

The ratio of the number of hydrogen-bonding single silanols to the number of hydrogen-bonding geminal silanols on the surface of the Fisher silica evacuated at 25 °C is seen from the data shown in Table 1 to be about 17-to-1; and about 46% of the geminal silanols and 53% of the single silanols are not hydrogen bonded. The corresponding values for the surface of the Baker silica evacuated at 200 °C are 16-to-1, 47% and 58%, respectively. Any satisfactory model for the silica surface should be able to explain these results. The fact that single silanols on the same (111)-type face of a β-cristobalite structure are not hydrogen bonded to each other (*vide supra*) can easily account for 53−58% of the non-hydrogen-bonding single silanols on the surfaces of the Fisher and Baker silicas evauated at 25 and 200 °C, respectively; the remaining 47−42% hydrogen-bonded single silanols can be interpreted in terms of the β-cristobalite model, if one invokes the idea of intersections of individual (111)-type surface planes with other surface planes—(111)-type or (100)-type.[38]

Figure 5 represents the unit cell of β-cristobalite. If the cube represented in Figure 5 is *inside* the framework of a silica gel particle, and if position m in Figure 5 represents a missing silicon in an internal defect, then if each of the oxygen atoms that would have been bonded to silicon m in a perfect crystal is instead bonded to a hydrogen, there will be four single silanols with their **Si−O**H internuclear axes perpendicular to four different (111)-type planes (for simplicity in the discussion, we assume that the Si−O−Si angle is 180° instead of 147°),[2,40] and these four single silanols point toward each other tetrahedrally. The spatial relationship of each pair of such single silanols is similar to that of the inner pair of hydroxyl groups shown in Figures 4A and 4B (same row); they are expected to hydrogen bond with each other. In other words, when two

---

(38) Chuang, I-S., Maciel, G. E. *J. Non-Cryst. Solids* Submitted for publication.

(39) Wells, F. A. *Structural Inorganic Chemistry*, 5th ed.; Claredon Press: Oxford, U.K., 1984; p 1007.

(40) Reference 39, p 1006.

(111)-type planes intersect concavely, the single silanols situated at the intersection can hydrogen bond with each other across the intersection. Therefore, at such a defect position m inside the framework of silica gel, each single silanol will be involved in hydrogen bonding with the other three single silanols. If, in addition to a silicon missing at position m, silicon is also missing at position e or position g, then there will be six single silanols and one geminal silanol in this defect; the two hydroxyl groups of this geminal silanol can form hydrogen bonds with six single silanols, which corresponds to a 6:1 ratio of hydrogen-bonding single silanols to geminal silanols. Again, the spatial relationship of each pair of such a single silanol and its neighboring geminal silanols at the concave intersection of a (111)-type plane and a (100)-type plane is similar to that of the inner pair of hydroxyl groups shown in Figures 4A and 4B (same row); they can hydrogen bond with each other across the intersection. This kind of configuration could presumably be present on the outside surface and/or inside the bulk of silica gel.

One of our previous articles[17] indicated that all hydrogen-bonding single silanols and almost all geminal silanols (hydrogen-bonding or non-hydrogen-bonding) should be external, i.e., accessible to D_2O exchange. It was found that almost all hydroxyl groups inaccessible to D_2O exchange are non-hydrogen-bonding single silanols. Even though we do not rule out the possibility that one geminal silanol can be involved in hydrogen bonding with six single silanols and at the same time be accessible for D_2O exchange, we regard this defect configuration as only a minor population for hydrogen-bonding single silanols and geminal silanols. Other possible explanations for the experimentally determined relative numbers of hydrogen-bonding geminal silanols and single silanols are explored in the following paragraphs. We have already discussed the hydrogen-bonding possibilities between hydroxyl groups of geminal silanols on individual (100)-type silica surfaces (cf., Figure 4). If one considers the various kinds of intersections between (100)-type surface planes and (111)-type surface planes, then one finds various other possibilities for hydrogen bonding between hydroxyl groups of pairs of single silanols, and between hydroxyl groups of single silanols and geminal silanols on the silica surface.

According to the simple β-cristobalite model previously introduced for single silanols and geminal silanols on a silica surface,[38] based on (111)-type (Figures 3B and 6A) and (100)-type (Figures 4 and 6B) faces, respectively, the single silanols on the same (111)-type face should not be hydrogen bonded to each other. However, if a (111)-type face intersects concavely with a (100)-type face, those single silanols at the intersection can form hydrogen bonds with adjacent geminal silanols, as represented in shorthand fashion in Figures 6C and 6D. Similarly, Figure 6E represents in shorthand notation the situation in which two non-parallel (111)-type faces intersect concavely with each other. As discussed earlier,[38] two single silanols on the *same* (111)-type face of a β-cristobalite system cannot hydrogen bond with each other; however, hydrogen bonding between single silanols across the concave intersection of two (111)-type faces can occur in the kind of situation depicted in Figure 6E.

The kinds of detailed models of pore (or defect) structures that can be represented in terms of structures like that depicted in Figure 6H are consistent with the general idea that surface curvature can make hydrogen bonding possible in situations that would not be conducive to hydrogen bonding if the surface were “flat”. A qualitatively similar view has been discussed by Legrand and co-workers.[16]

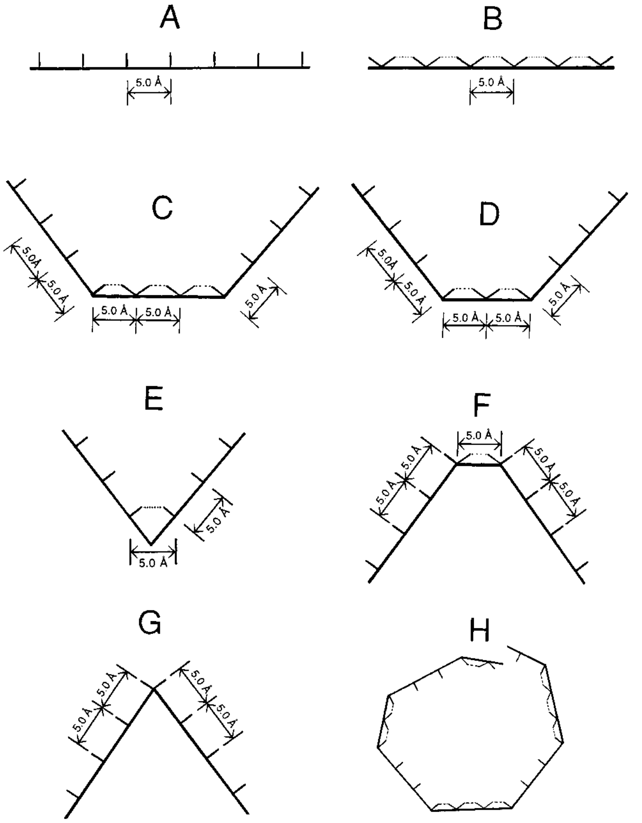

Figure 6. Parts A and B show shorthand notation for single (111)-type and (100)-type β-cristobalite faces, respectively, with short lines representing OH groups and long lines representing (111)-type and (100)-type faces of Figures 3B and 4A, respectively. Specific configurations are made possible by intersections of two (111)-type β-cristobalite faces with each other (E and G) or with a (100)-type face (C, D, and F), as represented by shorthand notation. (H) A hypothetical model of a defect structure or pore structure of silica, as represented by shorthand notation. Dotted lines represent hydrogen bonds.

If one represents the silica gel surface by a complex model of intersecting (100)-type and (111)-type β-cristobalite faces, as represented in Figure 6, then one can begin to interpret the NMR-based results on hydrogen-bonded and non-hydrogen-bonded silanols. Judging from the occurrence of 53−58% of non-hydrogen-bonding single silanols and 46−47% of non-hydrogen-bonding geminal silanols, and assuming *a priori* roughly the same probability for concave intersections (which provide hydrogen-bonding opportunities) and convex intersections (which do not) between different (111)-type faces or between a (111)-type face and a (100)-type face, the number of columns of geminal silanols corresponding to Figures 6C and 6D is probably very close to one for silica gel surfaces. Furthermore, the near 1-to-1 number ratio of hydrogen-bonding to non-hydrogen-bonding single silanols implies a large number of pores. This is consistent with the known characteristics of silica gel.

The β-cristobalite model of the silica surface can also account for the effects of 25 or 200 °C vacuum dehydration of silica gel on the ^{29}Si NMR data presented above. Figures 6F and 6G show the convex intersections of two non-parallel (111)-type faces with each other (Figure 6G) or with a (100)-type face (Figure 6F). According to our β-cristobalite silica surface model, for those single silanols on the same (111)-type face (Figure 6A) or at the convex intersection of (111)-type and (100)-type faces (Figure 6F), and for those columns of geminal silanols right at the convex intersection of two (111)-type faces (Figure 6G), hydrogen bonding with other silanols cannot occur.

However, on an untreated silica surface, these silanols form hydrogen bonds with bridging water, as depicted in Figure 3A. After a silica surface is evacuated at 25 or at 200 °C, all the physisorbed water has been eliminated from the surface and these silanols, which were initially hydrogen bonded to water, have become isolated silanols. On the other hand, for those single silanols at the concave intersection(s) of two (111)-type faces (Figure 6E), or of one (111)-type face and one (100)-type face (Figures 6C or 6D), hydrogen bonding can occur with other single silanols or with geminal silanols across the intersection(s). For those geminal silanols in the same row of a (100)-type plane, as shown in Figures 4 and 6B, or at the concave intersection(s) of one (100)-type plane and one (111)-type plane (Figures 6C and 6D), hydrogen bonding can occur with other geminal silanols or with single silanols across the intersection(s). The silanols which are hydrogen bonded to other silanol(s) can also form hydrogen bonds with bridging water on an untreated silica surface. After the elimination of physisorbed water from the silica surface, these initially hydrogen-bonded silanols are no longer hydrogen bonded to water; however, hydrogen bonding *between* silanols is not disturbed by the elimination of physisorbed water. Our model indicates that non-hydrogen-bonded silanols of an evacuated silica can be either single or geminal silanols, and hydrogen-bonded silanols (single or geminal) can participate in hydrogen bonding with single silanols and/or geminal silanols. Thus, our model is consistent with the experimental results presented above for untreated silicas or silicas evacuated at temperatures of 200 °C or lower.

The dehydration of silica under vacuum at temperatures between 200 and 500 °C involves additional kinds of issues, e.g., the splitting out of water as Si−O−Si bridges are formed, and has been studied by a variety of experiments.[2,7,8,17,19] As the temperature is raised within this range, hydrogen-bonded silanols (single or geminal) start to split out water to form low-strain Si−O−Si linkages—apparently, the stronger the hydrogen bonding between two silanols, the more facile the Si−O−Si formation. Single or geminal silanols that are not hydrogen bonded are essentially unaffected by evacuation in the 200 to 500 °C temperature range. When a silica is subjected to heating under vacuum at temperatures ≥ 600 °C, some of the non-hydrogen-bonded silanols begin to "readjust their positions" on the surface and are able to condense irreversibly to form highly-strained Si−O−Si linkages. The β-cristobalite model is also capable of accounting for this behavior. Such issues, and a more detailed examination of the primary issues considered in this paper, will be published elsewhere.[38]

Summary and Conclusions

From $^{1}H \rightarrow ^{29}Si$ cross-polarization spin dynamics, it is possible to distinguish hydrogen-bonded silanols from non-hydrogen-bonded silanols. All the silanols of two untreated silica gel samples are hydrogen bonded either to water molecules or to other silanols. After evacuation at 25 or at 200 °C, those silanols that were hydrogen bonded only to water molecules become isolated silanols (non-hydrogen-bonded silanols), which can be single silanols or geminal silanols. On a Fisher silica gel surface evacuated at 25 °C, 53% of the single silanols and 46% of the geminal silanols are not hydrogen bonded, and the ratio of the number of hydrogen-bonded single silanols to hydrogen-bonded geminal silanols is 17-to-1. On the surface of a Baker silica gel evacuated at 200 °C, 58% of the single silanols and 47% of geminal silanols are non-hydrogen-bonded; the ratio of the number of hydrogen-bonded single silanols to hydrogen-bonded geminal silanols is 16-to-1.

In the β-cristobalite model for the silica surface, single silanols are situated on (111)-type faces and geminal silanols are situated on (100)-type faces; and single silanols and geminal silanols can either be hydrogen-bonded or non-hydrogen-bonded, depending on their local structural environments. Single silanols on the same (111)-type face cannot be hydrogen bonded to each other, while neighboring geminal silanols on the same (100)-type face may or may not be hydrogen bonded to each other, depending on the relative orientation of their hydroxyl groups. The two hydroxyl groups on the same geminal silanol cannot form hydrogen bonds with each other due to an unfavorable geometrical arrangement. When one (111)-type face intersects concavely with a (100)-type face, the single silanols and geminal silanols at the intersection are in the same (100)-type face and can hydrogen bond with each other. When a (111)-type face intersects with a (100)-type face convexly, there are no hydrogen bonds between a single silanol and its neighboring geminal silanol. If two (111)-type planes intersect concavely, single silanols at the intersection will also be situated on the same (100)-type face and can hydrogen bond "across" the intersection. When two (111)-type faces intersect convexly, an array of geminal silanols are situated at the intersection, and no hydrogen bonds exist in this arrangement. All the hydrogen bonding silanols have a common feature; i.e., when any two silanols are hydrogen bonded to each other, the two silicon atoms containing them are also situated on a same (100)-type plane. The generalized β-cristobalite model can readily explain the reversible dehydration/rehydration behavior of silica heated below 500 °C, as well as the irreversible dehydration/rehydration behavior of silicas heated to temperatures above 600 °C.

Acknowledgment. The authors gratefully acknowledge partial support of this research by the National Science Foundation Grant No. CHE-9021003 and by Grant No. F49620-95-1-0192 from the Air Force Office of Scientific Research.

JA951550D